

ON HYPERBOLIC KNOTS REALIZING THE MAXIMAL DISTANCE BETWEEN TOROIDAL SURGERIES

MASAKAZU TERAGAITO

ABSTRACT. For a hyperbolic knot in the 3-sphere, the distance between toroidal surgeries is at most 5, except the figure eight knot. In this paper, we determine all hyperbolic knots that admit two toroidal surgeries with distance 5.

1. INTRODUCTION

Let K be a hyperbolic knot in the 3-sphere S^3 with exterior $E(K) = S^3 - \text{Int } N(K)$. For a slope r on $\partial E(K)$, $K(r)$ denotes the manifold obtained by r -surgery. That is, $K(r) = E(K) \cup V$, where V is a solid torus attached to $E(K)$ along $\partial E(K)$ in such a way that r bounds a meridian disk in V . By Thurston's hyperbolic Dehn surgery theorem [17], $K(r)$ is a hyperbolic 3-manifold, except at most finitely many slopes r . If $K(r)$ fails to be hyperbolic, then it is conjectured that $K(r)$ is a Seifert fibered manifold or a toroidal manifold [6]. A 3-manifold is said to be *toroidal* if it contains an essential torus. If $K(r)$ is toroidal, then the slope r (or the surgery) is said to be *toroidal*. By [7], a toroidal slope corresponds to an integer or a half-integer under the standard parameterization of slopes by the set $\mathbb{Q} \cup \{1/0\}$ (see [14]). In other words, a toroidal slope runs at most twice along the knot. Eudave-Muñoz [2] constructed an infinite family of hyperbolic knots, denoted by $k(\ell, m, n, p)$ in his notation, each of which admits a half-integral toroidal surgery. In fact, Gordon and Luecke [8] proved that these are the only knots that admit half-integral toroidal surgery.

Let $\Delta(r, s)$ denote the distance between slopes r and s . That is, it is the minimal geometric intersection number between r and s . As it is well known [6], the figure eight knot admits exactly three toroidal slopes $-4, 0$ and 4 . Notice that $\Delta(-4, 4) = 8$. For convenience, assume that K is not the figure eight knot. Then the distance between toroidal slopes of K is at most 5 by [5], and one between integral toroidal slopes is at most 4 by [15]. Thus we see that if K admits two toroidal slopes at distance 5 then one slope is half-integral, and therefore K is one of Eudave-Muñoz knots $k(\ell, m, n, p)$. In fact, any $k(2, -1, n, 0)$, for $n \neq 1$, admits two toroidal slopes $25n - 16$ and $25n - 37/2$ of distance 5 [3]. We remark that $k(2, -1, n, 0)$ is obtained from the trefoil component of the Whitehead sister link (the $(-2, 3, 8)$ -pretzel link) by doing $-1/(n-1)$ -surgery along the unknotted component, and that $k(2, -1, 1, 0)$ is the trefoil and $k(2, -1, 0, 0)$ is the mirror image of the $(-2, 3, 7)$ -pretzel knot. The purpose of this paper is to prove that these are the only hyperbolic knots that realize distance 5 between toroidal slopes.

2000 *Mathematics Subject Classification.* Primary 57M25.

Key words and phrases. knot, Dehn surgery, toroidal surgery.

Partially supported by Japan Society for the Promotion of Science, Grant-in-Aid for Scientific Research (C), 16540071.

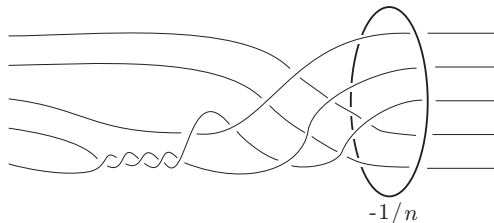


FIGURE 1.

Theorem 1.1. *Let K be a hyperbolic knot in S^3 . If K admits two toroidal slopes α and β with $\Delta(\alpha, \beta) = 5$, then K is the Eudave-Muñoz knot $k(2, -1, n, 0)$ for some integer $n \neq 1$, and $\{\alpha, \beta\} = \{25n - 16, 25n - 37/2\}$.*

In Figure 1, the knot $k(2, -1, n, 0)$, expressed in a braid form, is obtained after $-1/n$ -surgery along the unknotted circle. This is directly obtained from [2, Figure 24]. Notice that $k(2, -1, n_1, 0)$ and $k(2, -1, n_2, 0)$ are not equivalent if $n_1 \neq n_2$, since any knot admits at most one half-integral toroidal slope [11].

Among the toroidal slopes listed in [2], the distance 5 is realized only by the knots in our Theorem 1.1. If the list of [2] is complete, then our Theorem would be its consequence. But it seems to be hard to confirm the completeness, and hence we will take another approach. As in [6, 15], we consider the labelled intersection graphs on two essential tori in the surgered manifolds.

It is conjectured that a hyperbolic knot in S^3 has at most 3 toroidal slopes [2] (see also [12, Problem 1.77 A(5)]). In [15], we gave an upper bound 5 for the number of toroidal slopes. Theorem 1.1 implies that the conjecture holds for Eudave-Muñoz knots.

Corollary 1.2. *Any Eudave-Muñoz knot admits at most 3 toroidal slopes.*

Proof. Let $K = k(\ell, m, n, p)$ be an Eudave-Muñoz knot. Then K has the unique non-integral toroidal slope r by [11]. Let $s = r + 1/2$. Then the slopes $s - 1$ and s yield atoroidal Seifert fibered manifolds [2, 3].

If K is not equivalent to $k(2, -1, n, 0)$, then the distance between two toroidal slopes is at most 4 by Theorem 1.1. Hence $\{s - 2, r, s + 1\}$ gives the set of possible toroidal slopes. If $K = k(2, -1, n, 0)$, then $s = 25n - 18$ and $s + 1$ yields an atoroidal Seifert fibered manifold [3]. Hence $\{s - 2, r, s + 2\} = \{25n - 20, 25n - 37/2, 25n - 16\}$ is the set of possible toroidal slopes. \square

In Section 2, we collect basic facts for the analysis of the pair of graphs. In Sections 3 and 4, we will show that there is only one possible pair for the graphs realizing the distance 5. Finally, we prove that the pair determines the knot by using the construction of [8] in Section 5.

2. PRELIMINARIES

Let K be a hyperbolic knot. Assume that K admits two toroidal slopes α and β with distance 5. Then one of the slopes is half-integral by [15]. Hence we assume that β is half-integral. By [8], we know that K is one of Eudave-Muñoz knots. Notice that $K(\alpha)$ and $K(\beta)$ are irreducible by [13, 18]. For the attached solid torus V_r of $K(r)$ where $r \in \{\alpha, \beta\}$, K_r denotes the core of V_r .

Let \widehat{S} be an essential torus in $K(\alpha)$.

Lemma 2.1. \widehat{S} is separating in $K(\alpha)$.

Proof. If not, $\alpha = 0$ by homological reason. Thus $K(0)$ contains a non-separating torus, and then K has genus one by [4]. But a genus one knot does not have half-integral toroidal surgery [16]. \square

We can assume that \widehat{S} intersects the attached solid torus V_α of $K(\alpha)$ in a disjoint union of s meridian disks, u_1, u_2, \dots, u_s numbered successively along V_α , and that s is minimal among all essential tori in $K(\alpha)$. By Lemma 2.1, s is even. Let $S = \widehat{S} \cap E(K)$. Then S is an incompressible and boundary-incompressible, punctured torus properly embedded in $E(K)$, each of whose boundary components has slope α on $\partial E(K)$.

Lemma 2.2. $K(\beta)$ does not contain a Klein bottle.

Proof. Since β is not integral, this follows from [7, Theorem 1.3]. \square

Let \widehat{T} be an essential torus in $K(\beta)$. Then \widehat{T} is separating and we can assume that \widehat{T} intersects the attached solid torus V_β in just two meridian disks v_1 and v_2 [7]. Let $T = \widehat{T} \cap E(K)$. Then T is an incompressible and boundary-incompressible, twice-punctured torus properly embedded in $E(K)$, where each component of ∂T has slope β .

We can assume that S and T intersect transversely, and that no arc component of $S \cap T$ is parallel to ∂S in S or ∂T in T . Also, we can assume that no circle component of $S \cap T$ bounds a disk in S or T by the incompressibility of S and T , and that ∂u_i meets ∂v_j in 5 points for any pair of i and j .

If we choose a basis $\{\mu, \alpha\}$ for $H_1(\partial E(K))$, where μ is the meridian of K , then β can be represented by $2\alpha \pm 5\mu$, since $\Delta(\mu, \beta) = 2$ and $\Delta(\alpha, \beta) = 5$. (This fact is called that the jumping number between α and β is two in the literature [6, 10].)

Lemma 2.3. Let a_1, a_2, a_3, a_4, a_5 be the points in $\partial u_i \cap \partial v_j$, numbered successively along ∂u_i . Then these points appear in the order of a_1, a_3, a_5, a_2, a_4 in some direction on ∂v_j . In other words, two points in $\partial u_i \cap \partial v_j$ are adjacent on ∂u_i if and only if they are not adjacent on ∂v_j , and vice-versa.

Proof. This follows from [10, Lemma 2.10]. \square

In the usual way [1, 6], we obtain two graphs G_S on \widehat{S} and G_T on \widehat{T} . More precisely, G_S has s vertices u_1, u_2, \dots, u_s , and G_T has two vertices v_1 and v_2 . The edges are the arc components of $S \cap T$. Note that neither graph has a trivial loop. An endpoint of an edge e in G_S at u_i has label j if it is in $\partial u_i \cap \partial v_j$. Thus the pair of labels 1 and 2 appears 5 times around u_i . Similarly, the endpoints of edges in G_T are labelled, and then the sequence of labels 1, 2, \dots , s appears 5 times around v_j . An edge is called a $\{i, j\}$ -edge if it has labels i and j at its endpoints.

Let $G = G_S$ or G_T . An edge of G is said to be *positive* if it connects two vertices (possibly, the same vertex) with the same parity. Otherwise, it is said to be *negative*. We denote by G^+ the subgraph of G consisting of all vertices and positive edges of G .

A subgraph H of G on a torus F is said to have an *annulus support* if there is an annulus A on F such that $H \subset \text{Int } A$ and a core of A is essential on F , and there is no disk on F containing H .

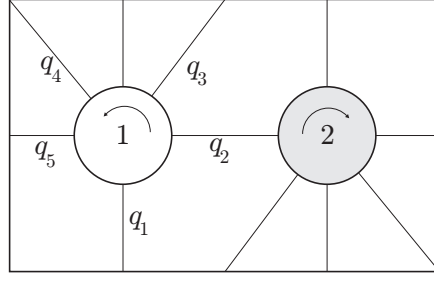


FIGURE 2.

A cycle in G is called a *Scharlemann cycle* if it bounds a disk face of G and all the edges are positive $\{i, i + 1\}$ -edges for some i . The pair of labels $\{i, i + 1\}$ is called the *label pair* of the Scharlemann cycle. In particular, a Scharlemann cycle consisting of two edges is called an *S-cycle* in short.

- Lemma 2.4.**
- (1) *No two edges can be parallel in both graphs.*
 - (2) (The parity rule) *An edge is positive in one graph if and only if it is negative in the other.*
 - (3) *If ρ is a Scharlemann cycle in G_S (resp. G_T), then its edges cannot lie in a disk on \widehat{T} (resp. \widehat{S}). In particular, if ρ is an S-cycle, then its edges form a cycle with an annulus support in the other graph.*

Proof. (1) is [5, Lemma 2.1]. (2) can be found in [1, p.279]. (3) is [7, Lemma 3.1] (Recall that $K(\alpha)$ and $K(\beta)$ are irreducible.) \square

The *reduced graph* \overline{G} of G is obtained from G by amalgamating each family of parallel edges into a single edge. For an edge e of \overline{G} , the *weight* of e is the number of edges in the corresponding family of parallel edges in G . In particular, \overline{G}_T is a subgraph of the graph in Figure 2, where the sides of the rectangle are identified to form the torus \widehat{T} in the usual way ([5, Lemma 5.2]). Also, q_i denotes the weight of an edge. Notice that v_1 and v_2 are incident to the same number of loops in G_T . Since G_T is determined by non-negative integers q_i , we say $G_T \cong G(q_1, q_2, q_3, q_4, q_5)$. Let Q_i denote the family of parallel edges in G_T with weight q_i for $i = 2, 3, 4, 5$.

Lemma 2.5. G_S satisfies the following.

- (1) *Any family of parallel positive edges contains at most 3 edges.*
- (2) *Any family of parallel negative edges contains at most two edges.*

Proof. (1) If there are 4 parallel positive edges in G_S , then there are two bigons among them which lie on the same side of \widehat{T} . By Lemma 2.4(1), these 4 edges belong to mutually distinct families of parallel negative edges in G_T . But this implies that $K(\beta)$ contains a Klein bottle (see the proof of [9, Lemma 5.2]), which contradicts Lemma 2.2.

(2) Any negative edge in G_S corresponds to a loop at v_1 or v_2 in G_T by the parity rule. The result follows from that any two loops at v_i are parallel and Lemma 2.4(1). \square

Lemma 2.6. G_T satisfies the following.

- (1) *If $s = 4$, then there are no two S-cycles with disjoint label pairs.*

- (2) If $s \geq 4$, then any family of parallel positive edges contains at most $s/2 + 1$ edges. Moreover, if it contains $s/2 + 1$ edges, then two adjacent edges on one end form an S -cycle.
- (3) Any family of parallel negative edges contains at most s edges.
- (4) The faces of two S -cycles with disjoint label pairs lie on the same side of \widehat{S} .

Proof. (1) Let ρ_1 and ρ_2 be S -cycles with disk faces f_1 and f_2 , and label pairs $\{1, 2\}$ and $\{3, 4\}$, say. Let H_{12} and H_{34} be the parts of V_α between u_1 and u_2 , u_3 and u_4 , respectively. Then shrinking V_{12} radially to its core in $V_{12} \cup f_1$ gives a Möbius band B_1 such that ∂B_1 is the loop on \widehat{S} formed by the edges of ρ_1 . Similarly, we obtain another Möbius band B_2 whose boundary is disjoint from ∂B_1 . Let A be an annulus between ∂B_1 and ∂B_2 on \widehat{S} . Then $B_1 \cup A \cup B_2$ is a Klein bottle \widehat{F} in $K(\alpha)$, which meets the core of V_α in two points (after a perturbation). Then $F = \widehat{F} \cap E(K)$ gives a twice-punctured Klein bottle in $E(K)$. By attaching a suitable annulus on $\partial E(K)$ to F along their boundaries, we obtain a closed non-orientable surface in S^3 , a contradiction.

(2) By [18, Lemma 1.4], such family contains at most $s/2 + 2$ edges. Furthermore, if it contains $s/2 + 2$ edges, then we can assume that there are two S -cycles with disjoint label pairs $\{1, 2\}$ and $\{s/2 + 1, s/2 + 2\}$ in the family (see [18, Figure 1]). By the same construction as in (1), we have two Möbius bands B_1 and B_2 and an annulus A on \widehat{S} . In \widehat{S} , two vertices u_i and u_{s-i+3} are connected by an edge in the family for $i = 3, 4, \dots, s/2$. Hence $\text{Int } A$ contains an even number of vertices. Then $B_1 \cup A \cup B_2$ is a Klein bottle which meets V_α in an even number of meridian disks. This leads to a contradiction as before.

If the family contains $s/2 + 1$ edges, then it contains an S -cycle at one end [18, Lemma 1.4].

(3) If $s \geq 4$, then this is [10, Lemma 2.3(1)]. If $s = 2$, then any negative edge in G_T has the same label at its endpoints. Thus if a family of parallel negative edges contains 3 edges, then there would be two edges which are parallel in both graphs. This contradicts Lemma 2.4.

(4) is [18, Lemma 1.7]. □

Suppose $q_i = s$. Let e_1, e_2, \dots, e_s be the edges of Q_i , numbered successively. We may assume that e_j has label j at v_1 for $1 \leq j \leq s$. Then these edges defines a permutation σ of the set $\{1, 2, \dots, s\}$ such that e_j has label $\sigma(j)$ at v_2 . In fact, $\sigma(j) \equiv j + k \pmod{s}$ for some even k . This σ is called the *associated permutation* to Q_i . By the parity rule, σ has at least two orbits, and all orbits have the same length. According to the orbits of σ , the edges of Q_i form disjoint cycles on \widehat{S} .

Lemma 2.7. *Each of these cycles is essential on \widehat{S} .*

Proof. This is [6, Lemma 2.3]. □

3. THE CASE THAT $s \geq 4$

In this section, we will show that the case where $s \geq 4$ is impossible. Recall that $q_1 \leq s/2 + 1$ and $q_i \leq s$ for $i \geq 2$ by Lemma 2.6.

Lemma 3.1. $q_1 = s/2$ or $s/2 + 1$.

Proof. Since $2q_1 + q_2 + q_3 + q_4 + q_5 = 5s$, $q_1 \geq s/2$. The result follows from this. □

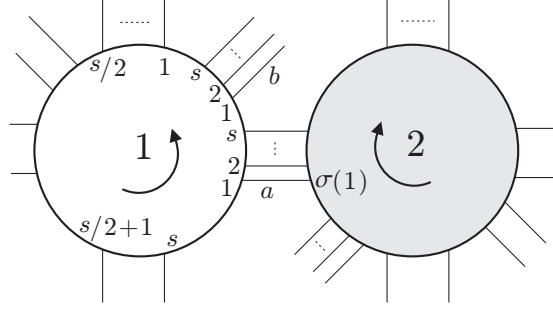


FIGURE 3.

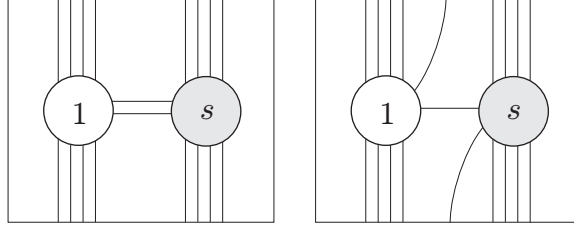


FIGURE 4.

We distinguish two cases.

3.1. $q_1 = s/2$. Then $G_T \cong G(s/2, s, s, s, s)$. We can assume that G_T has labels as in Figure 3.

Let σ be the associated permutation to Q_2 such that an edge in Q_2 has label i at v_1 and label $\sigma(i)$ at v_2 . Notice that the associated permutations to Q_3, Q_4 and Q_5 are equal to σ .

Lemma 3.2. σ is not the identity.

Proof. Suppose that σ is the identity. Then each vertex of G_S is incident to 4 loops. Let $G(1, s)$ be the subgraph of G_S spanned by u_1 and u_s . Since $s \geq 4$, $G(1, s)$ has an annulus support on \widehat{S} , and there are only two possibilities for it as in Figure 4, where the top and bottom edges are identified to form an annulus.

Let a be the $\{1, 1\}$ -edge in Q_2 , and let a_i be its endpoint at v_i for $i = 1, 2$. Let e (resp. f) be the $\{1, s\}$ -loop at v_1 (v_2), and let e_1 and f_1 be their endpoints with label 1. Around v_1 , a_1 and e_1 are not successive among 5 occurrences of label 1, but a_2 and f_1 are successive among 5 occurrences of label 1 around v_2 . By Lemma 2.3, a_1 and e_1 are successive among 5 occurrences of label 1 around u_1 , but a_2 and f_1 are not successive among 5 occurrences of label 2 around u_1 . But this is not satisfied in both configurations of Figure 4. \square

Lemma 3.3. σ^2 is the identity. In particular, each orbit of σ has length two, and $\sigma(i) = i + s/2$.

Proof. The edges of Q_2 form disjoint cycles in G_S according to the orbits of σ , and such cycle is essential on \widehat{S} by Lemma 2.7. Recall that there are at least two such

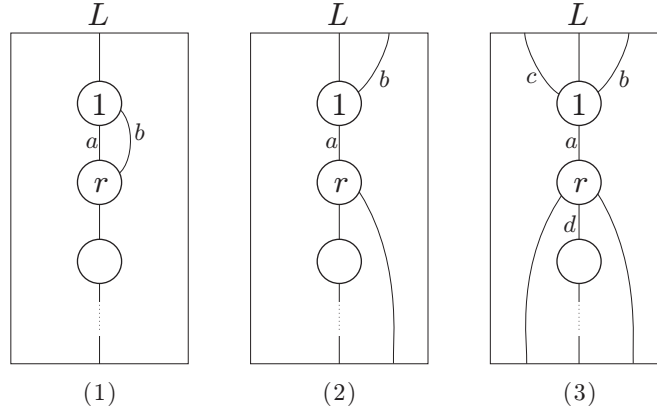


FIGURE 5.

cycles. Let L be the cycle corresponding to the orbit of σ containing 1. Let a and b be the edges of Q_2 and Q_3 with label 1 at v_1 , respectively (see Figure 3). Then $L \cup b$ has an annulus support on \widehat{S} . Thus there are two possibilities for $L \cup b$ as in Figure 5(1) and (2), where $r = \sigma(1)$. Note that a and b have label 1 at u_1 .

For Figure 5(1), there is another edge e between a and b . Then e is a negative $\{1, r\}$ -edge in G_T with label r at v_1 and label 1 at v_2 . Although e need not be in Q_2 , this implies $\sigma(r) = 1$, because any family of negative parallel edges has the same permutation σ . Hence σ^2 is the identity.

For Figure 5(2), let c and d be the edges of Q_4 and Q_5 with label 1 at v_1 , respectively. Then there would be a pair of parallel edges among a, b, c, d on \widehat{S} . Thus the above argument gives the conclusion. \square

Lemma 3.4. *The case $q_1 = s/2$ is impossible.*

Proof. By Lemma 3.3, G_S^+ consists of $s/2$ components, each of which has an annulus support. In fact, any component consists of two vertices and 8 edges. Thus there are at least 4 mutually parallel positive edges. But this is impossible by Lemma 2.5(1). \square

3.2. $q_1 = s/2 + 1$. Since $q_2 + q_3 + q_4 + q_5 = 4s - 2$, at least two of q_i are s . By the parity rule, $q_2 + q_3$ and $q_4 + q_5$ are even. Thus we may assume that $G_T \cong G(s/2 + 1, s, s, s, s - 2)$ or $G(s/2 + 1, s, s, s - 1, s - 1)$ without loss of generality.

Lemma 3.5. *$G(s/2 + 1, s, s, s - 1, s - 1)$ is impossible.*

Proof. Assume $G_T \cong G(s/2 + 1, s, s, s - 1, s - 1)$. By the parity rule, each edge of Q_2 has labels of the same parity. But then each edge of Q_4 has labels of opposite parities at its ends. This contradicts the parity rule. \square

Thus $G_T \cong G(s/2 + 1, s, s, s, s - 2)$. We can assume that the edges of Q_2 have labels $1, 2, \dots, s$ at v_1 as in Figure 3. Then there is an S -cycle with label pair $\{s/2, s/2 + 1\}$ among loops at v_1 . Let σ be the associated permutation to Q_2 as before. Notice that Q_3 and Q_5 also associate to σ . (Although $q_5 = s - 2$, the associated permutation is obviously defined.)

Lemma 3.6. *σ is the identity.*

Proof. Among loops at v_2 , there is an S -cycle with label pair $\{r + s/2 - 1, r + s/2\}$, where $r = \sigma(1)$. Assume that σ is not the identity. Then r is odd by the parity rule, and $r \geq 3$.

If $s = 4$, then $r = 3$. Hence G_T contains two S -cycles with label pairs $\{2, 3\}$ and $\{4, 1\}$. But this contradicts Lemma 2.6. Hence $s > 4$.

We claim that σ^2 is the identity. To see this, assume not. As in the proof of Lemma 3.3, the edges of Q_2 form disjoint cycles according to the orbits of σ . Let L be the cycle through u_1 . Notice that L contains at least three vertices. Let a and b be the edges of Q_2 and Q_3 with label 1 at v_1 . Then $L \cup b$ has an annulus support. If b is parallel to a , then σ^2 would be the identity. Hence $L \cup b$ is as shown in Figure 5(2). Let c be the edge of Q_5 with label 1 at v_1 . If c is parallel to a or b on \widehat{S} , then σ^2 would be the identity again. Hence c is located as in Figure 5(3). Let d and e be the edges of Q_2 and Q_3 with label r at v_1 . Of course, d is in L . But e must be parallel to d . Hence σ^2 would be the identity, a contradiction.

Therefore $r = s/2 + 1$. Since r is odd, $s \equiv 0 \pmod{4}$. The edges of Q_2 form cycles of length two on \widehat{S} , and there are at least 4 such cycles. In particular, u_1 and $u_{s/2+1}$ lie on the same cycle, and so do $u_{s/2}$ and u_s .

Also, G_T contain two S -cycles with label pairs $\{s/2, s/2 + 1\}$ and $\{s, 1\}$. But we cannot locate the edges of these S -cycles to form essential cycles on \widehat{S} simultaneously. This contradicts Lemma 2.4(3). \square

Lemma 3.7. $s = 4$.

Proof. Assume $s > 4$. Notice that the associated permutation τ to Q_4 is defined as $\tau(i) = i - 2$. Hence the edges of Q_4 form two cycles on \widehat{S} , each of which contains at least three vertices. By Lemma 3.6, each vertex of G_S is incident to a loop. Hence there would be a trivial loop. \square

Lemma 3.8. *The case $q_1 = s/2 + 1$ is impossible.*

Proof. In G_S , u_1 and u_4 are incident to 3 loops respectively, and u_2 and u_3 are incident to two loops. Also, G_T contains two S -cycles with label pair $\{2, 3\}$. The edges of them give 4 edges between u_2 and u_3 in G_S . There are two edges between u_1 and u_3 , which belong to Q_4 in G_T . Hence they are not parallel in G_S by Lemma 2.4.

Let a, b, d, e be the edges of Q_2, Q_3, Q_4, Q_5 with label 1 at v_1 . Also, let c be the loop at v_1 with label 1. By Lemma 2.3, these edges appear in the order a, c, e, b, d around u_1 in some direction. Let f be the edge of Q_4 with label 3 at v_1 . Then the endpoints of b and f at v_2 are consecutive among 5 occurrences of label 1. Also, their endpoints at u_1 are consecutive among 5 occurrences of label 2. This contradicts Lemma 2.3. \square

4. THE CASE THAT $s = 2$

In this section, we show that there is only one possible pair of the graphs, which will lead to the determination of knots in the next section.

The reduced graphs \overline{G}_S and \overline{G}_T are subgraphs of the graph as shown in Figure 2. We use p_i (resp. q_i) to denote the weight of edge in \overline{G}_S (resp. \overline{G}_T). In Figure 2, q_i is indicated, but p_i is assigned at the same place as q_i . Also, we say $G_S \cong G(p_1, p_2, p_3, p_4, p_5)$, similarly to G_T . Recall that $p_1 \leq 3$ and $p_i \leq 2$ for $i = 2, 3, 4, 5$ by Lemma 2.5. Since $2p_1 + p_2 + p_3 + p_4 + p_5 = 10$, $p_1 \geq 1$.

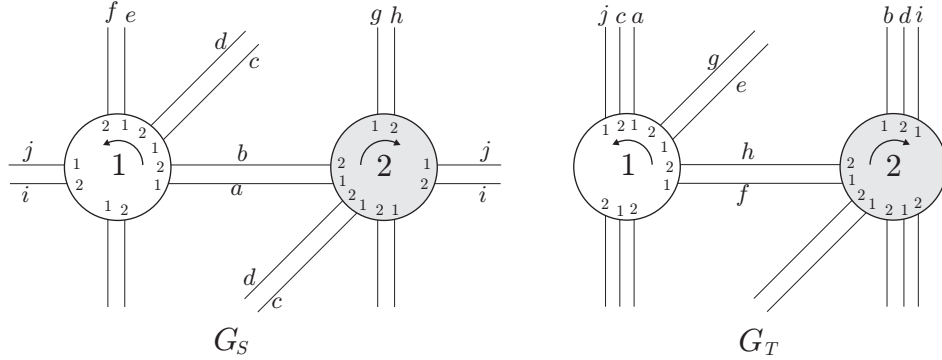


FIGURE 6.

Lemma 4.1. $p_1 = 1$ is impossible.

Proof. If $p_1 = 1$, then $p_i = 2$ for any $i \neq 1$. Then $G_T \cong G(4, 2, 0, 0, 0)$ or $G(4, 1, 1, 0, 0)$. But these are eliminated as in the proof of Lemma 3.2. \square

Thus $p_1 = 2$ or 3.

Lemma 4.2. If $p_1 = 2$, then the graphs are as shown in Figure 6. The correspondence between the edges in G_S and G_T is uniquely determined up to symmetry.

Proof. Suppose $p_1 = 2$. By the parity rule, $p_2 + p_3 + 3$ and $p_4 + p_5$ is even. Hence we can assume that $p_2 + p_3 = 4$ and $p_4 + p_5 = 2$. Then $p_2 = p_3 = 2$ by Lemma 2.5. If $p_4 = p_5 = 1$, then the labels in G_S contradicts the parity rule. Thus we can assume that $G_S \cong G(2, 2, 2, 2, 0)$, and then there are 4 possibilities for G_T up to symmetry as in Figure 7.

(3) contradicts the parity rule.

To eliminate (1) and (2), notice that G_S contains two S -cycles ρ_1 and ρ_2 whose faces lie on the same side of \widehat{T} . From the labeling of G_S , we can determine the edges of ρ_i in G_T as in Figure 8, respectively. For (1), let D_i be the disk face bounded by ρ_i , and let H be the annulus in ∂V_β between v_1 and v_2 , meeting ∂D_i . Then $\partial D_1 \cup \partial D_2$ splits H into 4 rectangles. By attaching suitable two rectangles to D_1 and D_2 , respectively, we obtain two Möbius bands B_1 and B_2 , whose boundaries are disjoint on \widehat{T} . Thus $K(\beta)$ would contain a Klein bottle as the union of B_1 , B_2 and an annulus on \widehat{T} , a contradiction. For (2), it is impossible to connect these 4 edges of ρ_i on ∂V_β simultaneously.

For (4), the edge correspondence is determined in the same way as [10, Lemma 5.3] by using the fact that the jumping number is two. Notice that this pair coincides with that of [10, Figures 5.2(e) and 5.3(b)], when G_T is regarded as a graph in an annulus. \square

Lemma 4.3. If $p_1 = 3$, then the graphs are the same as in Figure 6 with exchanging G_S and G_T .

Proof. We may assume that $(p_2 + p_3, p_4 + p_5) = (2, 2)$ or $(4, 0)$ by symmetry. In the former case, there are three possibilities for G_S , up to equivalence, as shown in Figure 7(1), (2) and (3).

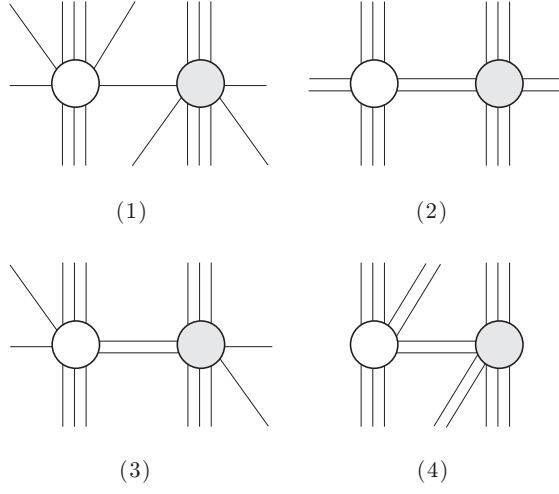


FIGURE 7.

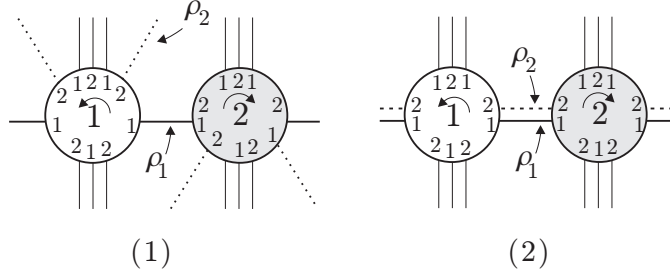


FIGURE 8.

(3) is impossible by the parity rule. If G_S is (2), then the labeling of G_S implies that G_T contains an S -cycle at each vertex. It is easy to see that their faces lie on the same side of \widehat{S} . In fact, $G_T \cong G(2, 2, 2, 2, 0)$. Hence the argument in the proof of Lemma 4.2 works again (with an exchange of roles between G_S and G_T). If G_S is (1), then the endpoints of two $\{1, 1\}$ negative edges at u_1 are not successive among 5 occurrences of label 1. Hence Lemma 2.3 implies that $(q_2 + q_3, q_4 + q_5) = (6, 0)$, up to symmetry. But this is impossible since $q_i \leq 2$ for $i \neq 1$.

Thus $(p_2 + p_3, p_4 + p_5) = (4, 0)$, giving $p_2 = p_3 = 2$. Hence $q_1 = 2$, and so we can assume that $(q_2 + q_3, q_4 + q_5) = (6, 0)$ or $(4, 2)$. But $(6, 0)$ is impossible again. By using the parity rule, it is easy to see that G_T is as in Figure 6 (with exchanging G_S and G_T). \square

We have thus shown that there is only one possibility for the pair $\{G_S, G_T\}$ realizing the distance 5, as shown in Figure 6 (or with an exchange of G_S and G_T).

5. DETERMINING THE KNOT

In this section, we will show that the only possibility for $\{G_S, G_T\}$ corresponds to the Eudave-Muñoz knot $k(2, -1, n, 0)$. We follow the construction in [8, Section 5], and use the same notation as far as possible. We assume that the pair is as

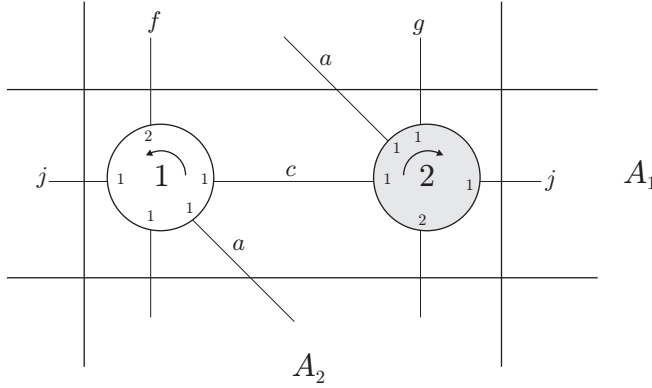


FIGURE 9.

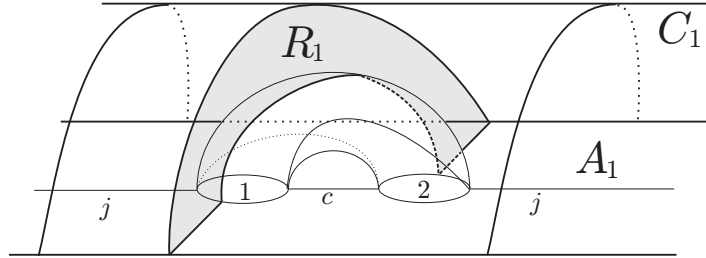


FIGURE 10.

in Figure 6 with exchanging G_S and G_T to fit the notation to [8]. As shown in Lemmas 4.2 and 4.3, G_S and G_T can be exchanged. Hence we cannot say which of α and β is non-integral with respect to the original framing of K in the following argument.

Let f_1 and f_2 be the bigons in G_S bounded by the edges c and j , a and c , respectively. Also, let f_3 be the 3-gon bounded by a, g and f . Up to homeomorphism, we can assume that these edges are as in Figure 9 on \widehat{T} . For $i = 1, 2$, let A_i be an annulus support of the edges of f_i , and let $A'_i = \text{cl}(\widehat{T} - A_i)$.

Let $K(\beta) = M_1 \cup_{\widehat{T}} M_2$, and let $H_i = V_\beta \cap M_i$. We may assume that f_i lies in M_i . Then $W_i = N(A_i \cup H_i \cup f_i) \subset M_i$ is a solid torus [7, Lemma 3.7], and moreover $M_i = W_i \cup W'_i$, where W'_i is a solid torus, is a Seifert fibered manifold over the disk with two exceptional fibers, one of which has index two [7, Lemma 3.8]. Let $\partial W_i = A_i \cup C_i$. Take a disk (rectangle) R_i in $\text{cl}(W_i - H_i)$ as in [8]. See Figures 10 and 11.

Now, regard $\widehat{T} \cup C_1 \cup C_2 \cup R_1 \cup R_2 \cup V_\beta$ as a subset of S^3 as follows. Embed \widehat{T} as a standard torus in S^3 , which splits S^3 into two solid tori U_1 and U_2 . We assume that the components of ∂A_1 are longitudes of U_1 , and those of ∂A_2 are meridians of U_1 . Then C_i is identified with the obvious annulus in U_i , separating U_i into two solid tori V_i and V'_i , where $\partial V_i = A_i \cup C_i$ and $\partial V'_i = A'_i \cup C_i$. Finally, embed V_β in the obvious way, and R_i as in Figures 10 and 11.

Let K_i be a core of V_i disjoint from $H_i \cup R_i$, and let K'_i be a core of V'_i . Notice that $N(\widehat{T} \cup C_1 \cup C_2)$ is the exterior of the link $L_0 = K_1 \cup K'_1 \cup K_2 \cup K'_2$. Since

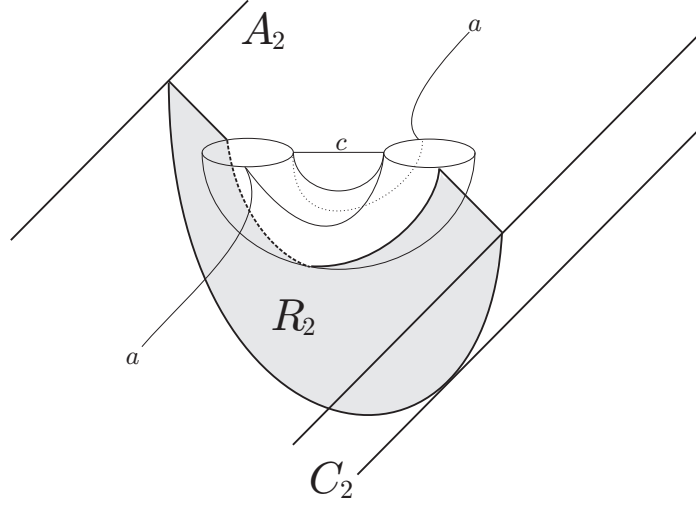


FIGURE 11.

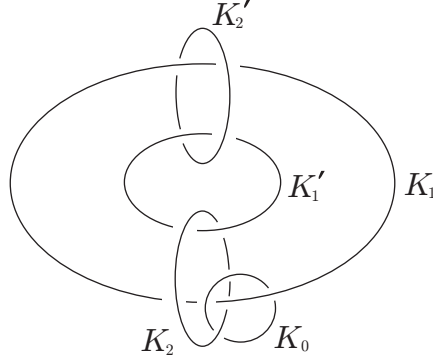


FIGURE 12.

W'_i is a solid torus, it is obtained from V'_i by some Dehn surgery on K'_i . Similarly, $(W_i; H_i, R_i)$ is obtained from $(V_i; H_i, R_i)$ by some Dehn surgery on K_i . Let K_0 be a core of $V_\beta \subset S^3$. Thus $(K(\beta), K_\beta)$ is obtained from (S^3, K_0) by some Dehn surgery on L_0 . In other words, $E(K)$ is obtained from $E(K_0)$ by Dehn surgery on L_0 . See Figure 12.

Lemma 5.1. *In the surgery description of $E(K)$ in Figure 12, $\alpha = -3/5$ and $\beta = 1/0$.*

Proof. This is obvious for β . For α , we draw ∂u_1 on V_β . See Figure 13. Thus $\alpha = -3/5$. \square

Lemma 5.2. *The filling slopes for (K_1, K'_1, K_2, K'_2) are $(-2, -3, -2, p/q)$, where $p/q \neq 0/1$.*

Proof. In Figure 10, it is easy to see that there is an annulus between ∂f_1 and the curve of slope $-2/1$ on $\partial N(K_1)$. This is similar for K_2 . Although we cannot

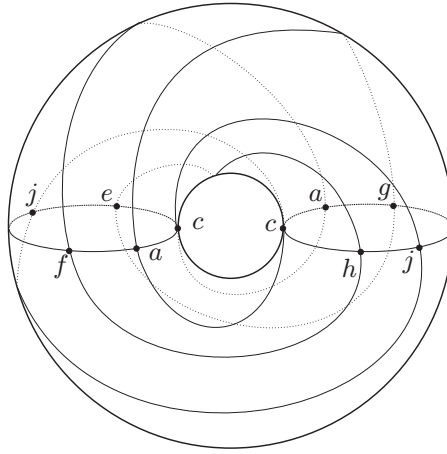


FIGURE 13.

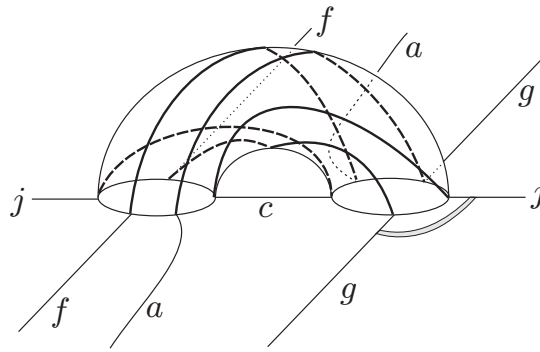


FIGURE 14.

determine the filling slope on K'_2 , it cannot be $0/1$, since a regular fiber of the Seifert fibration in M_2 is isotopic to a core of A_2 (see [7, Lemma 3.8]).

To determine the slope on K'_1 , we need the 3-gon f_3 . Notice that ∂f_3 is non-separating on $\partial W'_1$. Hence f_3 gives a meridian disk of W'_1 . Let f be the disk obtained by band summing f_3 and f_1 along the band on \widehat{T} as shown in Figure 14. Then it is easy to see that there is an annulus between ∂f and the curve of slope $-3/1$ on $\partial N(K'_1)$. \square

Lemma 5.3. *$E(K)$ has the surgery description as in Figure 15, where the filling slopes for (K'_1, K'_2) are $(4, (p + q)/q)$. Also, $\alpha = 3$ and $\beta = 1/2$ on K_0 .*

Proof. In the surgery description in Figure 12, perform a Kirby-Rolfsen calculus [14] in the following way (keeping the same symbols for the knots): a 1-twist on K_0 , a 1-twist on K_2 , and finally a 1-twist on K_1 . This sequence of twisting gives the surgery description of Figure 15. \square

Let μ be the meridian of K in S^3 .

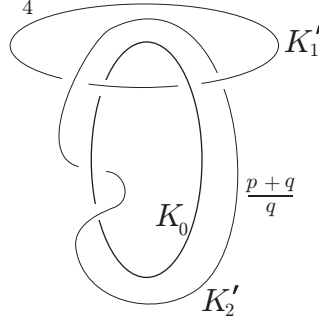


FIGURE 15.

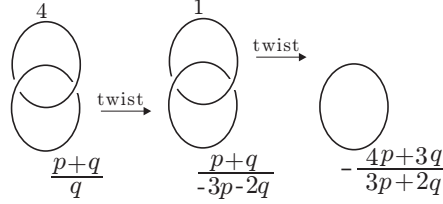


FIGURE 16.

Lemma 5.4. *If $\alpha \in \mathbb{Z}$ and $\beta \notin \mathbb{Z}$ with respect to the original framing of K , then $\mu = 1/0$ on K_0 in the surgery description of Figure 15. If $\alpha \notin \mathbb{Z}$ and $\beta \in \mathbb{Z}$, then $\mu = 1/1$.*

Proof. Let $\mu = m/n$ on K_0 in Figure 15. By Lemma 5.3, $\alpha = 3/1$ and $\beta = 1/2$ on K_0 . If $\alpha \in \mathbb{Z}$ and $\beta \notin \mathbb{Z}$ with respect to the original framing of K , then $\Delta(\mu, \alpha) = |3n - m| = 1$ and $\Delta(\mu, \beta) = |2m - n| = 2$. (Recall that β is half-integral.) This gives $(m, n) = (1, 0)$ or $(-1, 0)$. Hence $\mu = 1/0$.

If $\alpha \notin \mathbb{Z}$ and $\beta \in \mathbb{Z}$ with respect to the original framing of K , then a similar calculation shows that $(m, n) = (1, 1)$ or $(-1, -1)$. Thus $\mu = 1/1$. \square

Therefore, K can be identified with K_0 in Figure 15 when $\alpha \in \mathbb{Z}$ and $\beta \notin \mathbb{Z}$. Otherwise, K is the image of K_0 after a (-1) -twisting along K_0 .

Lemma 5.5. *If $\alpha \in \mathbb{Z}$ and $\beta \notin \mathbb{Z}$ with respect to the original framing of K , then $4p + 3q = \pm 1$. Otherwise, $4q - 3p = \pm 1$.*

Proof. Assume that $\alpha \in \mathbb{Z}$ and $\beta \notin \mathbb{Z}$. By Lemma 5.4, the surgery description of Figure 15, deleting K_0 , gives S^3 . A Kirby-Rolfsen calculus shows that this is equivalent to a trivial knot with framing $-(4p + 3q)/(3p + 2q)$ as in Figure 16. Hence $4p + 3q = \pm 1$.

When $\alpha \notin \mathbb{Z}$ and $\beta \in \mathbb{Z}$, first do a (-1) -twist on K_0 in Figure 15, and eliminate K_0 . This gives S^3 , and Figure 17 shows that this is equivalent to a trivial knot with framing $(4q - 3p)/(q - p)$. Hence $4q - 3p = \pm 1$. \square

Proof of Theorem 1.1. First assume that $\alpha \in \mathbb{Z}$ and $\beta \notin \mathbb{Z}$. We modify the surgery link of Figure 15 furthermore. After a (-3) -twisting along K'_2 , do a (-1) -twist along K'_1 . See Figure 18, where $K = K_0$ is expressed in a braid form. The framing

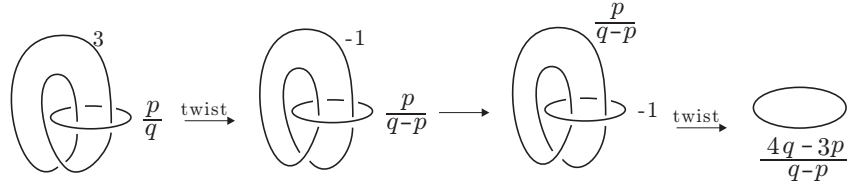


FIGURE 17.

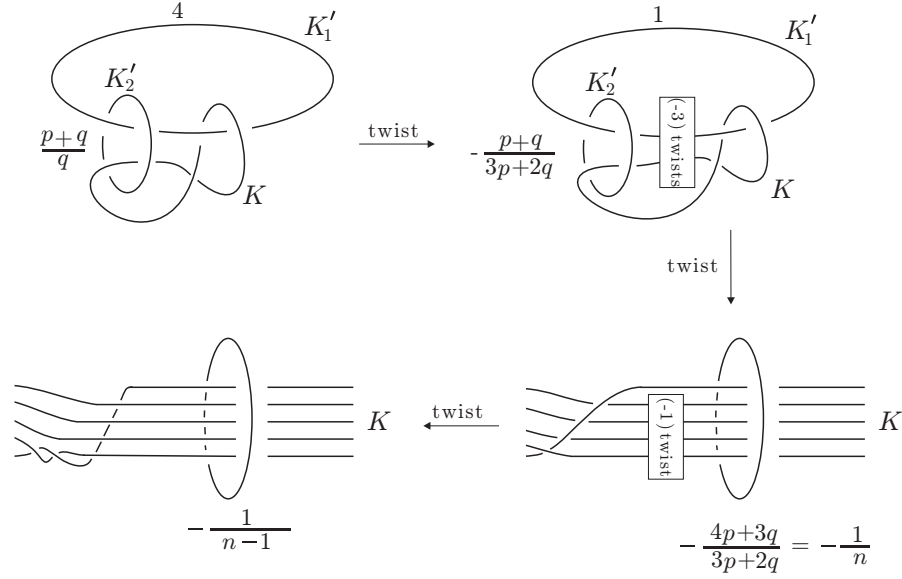


FIGURE 18.

on K'_2 is $-(4p + 3q)/(3p + 2q) = \pm 1/(3p + 2q)$ by Lemma 5.5, and $\alpha = -16$ and $\beta = -37/2$.

Put $n = (4p + 3q)(3p + 2q) = \pm(3p + 2q)$. After a 1-twisting along K'_2 , we have the Whitehead sister link, where the framing on the unknotted component is $-1/(n - 1)$. Hence $K = k(2, -1, n, 0)$, and $\alpha = 25n - 16$, $\beta = 25n - 37/2$. It is easy to see that $n \neq 1$ and n can take any other value.

Next, assume that $\alpha \notin \mathbb{Z}$ and $\beta \in \mathbb{Z}$. In this case, we perform a (-1) -twist along K_0 in Figure 15. Then $\mu = 1/0$ in the resulting surgery link, and so K can be identified with K_0 . Figure 19 starts from this link. At this point, $\alpha = -3/2$ and $\beta = 1$. After a (-1) -twist along K'_2 , do a 1-twist along K'_1 . Figure 19 shows only the last result, where the framing on K'_2 is $(4q - 3p)/(q - p) = \pm 1/(q - p)$ by Lemma 5.5, and $\alpha = 13/2$, $\beta = 9$. Again, this is the Whitehead sister link with the framing $\pm 1/(q - p)$ on the unknotted component. Hence $K = k(2, -1, n, 0)$, where $n = -(4q - 3p)(q - p) + 1 = \pm(q - p) + 1$, and $\alpha = 25n - 37/2$, $\beta = 25n - 16$. \square

ACKNOWLEDGEMENTS

The author would like to thank Mario Eudave-Muñoz for helpful conversations.

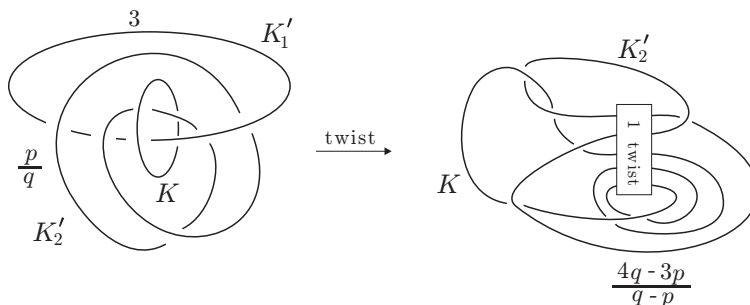


FIGURE 19.

REFERENCES

1. M. Culler, C. McA. Gordon, J. Luecke and P. Shalen, *Dehn surgery on knots*, Ann. of Math. **125** (1987), 237–300.
2. M. Eudave-Muñoz, *Non-hyperbolic manifolds obtained by Dehn surgery on hyperbolic knots*, Geometric topology (Athens, GA, 1993), 35–61, AMS/IP Stud. Adv. Math., 2.1, Amer. Math. Soc., Providence, RI, 1997.
3. M. Eudave-Muñoz, *On hyperbolic knots with Seifert fibered Dehn surgeries*, Topology Appl. **121** (2002), 119–141.
4. D. Gabai, *Foliations and the topology of 3-manifolds, III*, J. Differential Geom. **26** (1987), 479–536.
5. C. McA. Gordon, *Boundary slopes of punctured tori in 3-manifolds*, Trans. Amer. Math. Soc. **350** (1998), 1713–1790.
6. C. McA. Gordon, *Dehn filling: a survey*, Knot theory (Warsaw, 1995), 129–144, Banach Center Publ., 42, Polish Acad. Sci., Warsaw, 1998.
7. C. McA. Gordon and J. Luecke, *Dehn surgeries on knots creating essential tori, I*, Comm. Anal. Geom. **3** (1995), 597–644.
8. C. McA. Gordon and J. Luecke, *Non-integral toroidal Dehn surgeries*, Comm. Anal. Geom. **12** (2004), 417–485.
9. C. McA. Gordon and J. Luecke, *Toroidal and boundary-reducing Dehn fillings*, Topology Appl. **93** (1999), 77–90.
10. C. McA. Gordon and Y. Q. Wu, *Toroidal and annular Dehn fillings*, Proc. London Math. Soc. **78** (1999), 662–700.
11. C. McA. Gordon, Y. Q. Wu and X. Zhang, *Non-integral toroidal surgery on hyperbolic knots in S^3* , Proc. Amer. Math. Soc. **128** (2000), 1869–1879.
12. R. Kirby, *Problems in low-dimensional topology*, AMS/IP Stud. Adv. Math., 2.2, Geometric topology (Athens, GA, 1993), 35–473, Amer. Math. Soc., Providence, RI, 1997.
13. S. Oh, *Reducible and toroidal 3-manifolds obtained by Dehn fillings*, Topology Appl. **75** (1997), 93–104.
14. D. Rolfsen, *Knots and links*, Mathematics Lecture Series, **7**, Publish or Perish, Inc., Berkeley, Calif., 1976.
15. M. Teragaito, *Distance between toroidal surgeries on hyperbolic knots in the 3-sphere*, to appear in Trans. Amer. Math. Soc.
16. M. Teragaito, *Toroidal surgeries on hyperbolic knots, II*, Asian J. Math. **7** (2003), 139–146.
17. W. Thurston, *The geometry and topology of 3-manifolds*, Princeton University, 1978.
18. Y. Q. Wu, *Dehn fillings producing reducible manifolds and toroidal manifolds*, Topology **37** (1998), 95–108.

DEPARTMENT OF MATHEMATICS AND MATHEMATICS EDUCATION, HIROSHIMA UNIVERSITY, 1-1-1
 KAGAMIYAMA, HIGASHI-HIROSHIMA, JAPAN 739-8524
E-mail address: teragai@hiroshima-u.ac.jp